



# A Novel H<sub>2</sub>O<sub>2</sub> Generator for Tumor Chemotherapy-Enhanced CO Gas Therapy

Yang Li<sup>2†</sup>, Zeming Liu<sup>1†</sup>, Weng Zeng<sup>3†</sup>, Ziqi Wang<sup>4</sup>, Chunping Liu<sup>1</sup>, Ning Zeng<sup>1</sup>, Keli Zhong<sup>2\*</sup>, Dazhen Jiang<sup>5\*</sup> and Yiping Wu<sup>1\*</sup>

## OPEN ACCESS

### Edited by:

Husain Yar Khan,  
Wayne State University, United States

### Reviewed by:

Wei Wei,  
Memorial Sloan Kettering Cancer  
Center, United States  
Ting Zhuang,  
Xinxiang Medical University, China  
Jia Huang,  
Central South University, China

### \*Correspondence:

Keli Zhong  
zhongkeli@126.com  
Dazhen Jiang  
jiangdazhen@whu.edu.cn  
Yiping Wu  
wuyipingtj@163.com

<sup>†</sup>These authors have contributed  
equally to this work

### Specialty section:

This article was submitted to  
Pharmacology of  
Anti-Cancer Drugs,  
a section of the journal  
Frontiers in Oncology

Received: 09 July 2021

Accepted: 25 August 2021

Published: 21 September 2021

### Citation:

Li Y, Liu Z, Zeng W, Wang Z,  
Liu C, Zeng N, Zhong K, Jiang D  
and Wu Y (2021) A Novel H<sub>2</sub>O<sub>2</sub>  
Generator for Tumor Chemotherapy-  
Enhanced CO Gas Therapy.  
Front. Oncol. 11:738567.  
doi: 10.3389/fonc.2021.738567

<sup>1</sup> Department of Plastic Surgery, Tongji Hospital, Tongji Medical College, Huazhong University of Science and Technology, Wuhan, China, <sup>2</sup> Department of Gastrointestinal Surgery, Shenzhen People's Hospital (The Second Clinical Medical College, Jinan University, The First Affiliated Hospital, Southern University of Science and Technology), Shenzhen, China, <sup>3</sup> Department of Ophthalmology, Zhongnan Hospital of Wuhan University, Wuhan, China, <sup>4</sup> Key Laboratory of Artificial Micro- and Nano-Structures of Ministry of Education, School of Physics and Technology, Wuhan University, Wuhan, China, <sup>5</sup> Department of Radiation and Medical Oncology, Hubei Key Laboratory of Tumor Biological Behaviors, Hubei Cancer Clinical Study Center, Zhongnan Hospital of Wuhan University, Wuhan, China

Carbon monoxide (CO) gas therapy is a promising cancer treatment. However, gas delivery to the tumor site remains problematic. Proper tunable control of CO release in tumors is crucial to increasing the efficiency of CO treatment and reducing the risk of CO poisoning. To overcome such challenges, we designed ZCM, a novel stable nanotechnology delivery system comprising manganese carbonyl (MnCO) combined with anticancer drug camptothecin (CPT) loaded onto a zeolitic imidazole framework-8 (ZIF-8). After intravenous injection, ZCM gradually accumulates in cancerous tissues, decomposing in the acidic tumor microenvironment, releasing CPT and MnCO. CPT acts as a chemotherapy agent destroying tumors and producing copious H<sub>2</sub>O<sub>2</sub>. MnCO can react with the H<sub>2</sub>O<sub>2</sub> to generate CO, powerfully damaging the tumor. Both *in vitro* and *in vivo* experiments indicate that the ZCM system is both safe and has excellent tumor inhibition properties. ZCM is a novel system for CO controlled release, with significant potential to improve future cancer therapy.

**Keywords:** H<sub>2</sub>O<sub>2</sub> generator, CO gas therapy, camptothecin, ZIF-8 nanoparticles, TME (tumor microenvironment)

## INTRODUCTION

The targeted development of cancer treatment technology—including chemotherapy, radiotherapy, and immunotherapy—has enormous potential in tumor treatment, although most such technologies are yet to be used routinely in the clinic (1–5). Among therapeutic approaches being developed, treating cancer with CO gas is both novel and practical, yet remains underexplored. High-dose CO can reduce cell protein synthesis by inhibiting cellular mitochondrial respiration and induce cancer cell apoptosis (6–8). The safety and potency of CO therapy relies on the precise release of large amounts of CO directly into the tumor (8). However, most CO-related anticancer treatments are still in their initial stages, as the gaseous nature of CO makes controlled release highly problematic.

As a CO prodrug, manganese carbonyl (MnCO) has a Fenton-like reaction with  $H_2O_2$  to generate CO gas *in situ* (9). CO can then bind hemoglobin in tumor tissue, reducing its capacity for oxygen transport, causing mitochondrial damage, and thus achieving an anticancer effect without causing side effects systemically (9). Zhu and coworkers designed a novel type of CO delivery system using the immune evasion ability and tumor targeting of tumor-derived exosomes (EXO), encapsulating MnCO into exosomes by electroporation method to form the MMV system (6); this system could achieve a powerful antitumor effect in combination with low-dose radiotherapy. Both *in vivo* and *in vitro* experiments have verified the rationality of the MMV combined with RT designed by their team, and there is no inflammatory reaction and other side effects during the treatment period, which has good biological safety. Jin and his team used hollow mesoporous silica nanoparticle (hMSN) nanocarriers to effectively encapsulate MnCO and constructed a nano-drug (MnCO@hMSN) for antitumor research (10). After being internalized into the tumor tissue, the nanomedicine (MnCO@hMSN) will react with  $H_2O_2$  in the tumor (a new Fenton-like reaction that releases CO gas *in situ*) to achieve antitumor effects. *In vivo* experiments have shown that within the treatment cycle. The weight of the mice did not have any abnormalities, and the tumor proliferation was significantly inhibited (10). However, in cancer cells, although intracellular  $H_2O_2$  concentration can reach  $50 \mu M$ , endogenous  $H_2O_2$  is unable to achieve satisfactory efficiency (11–13). Insufficient  $H_2O_2$  in the tumor microenvironment (TME) is a profound problem for MnCO-based cancer therapy. CPT is a natural product topoisomerase inhibitor operating *via* several mechanisms including induction of cellular DNA damage (14–16). It is also an  $H_2O_2$  enhancer, inducing high levels of  $H_2O_2$  in the tumor (14). This property has interested several researchers. Tang et al. overcame the lack of target-specific, high-intensity luminescence by creating a target-specific chemiluminescence strategy, where CPT was loaded into the CLDRS system, enhancing  $H_2O_2$  concentration and chemiluminescence (14). However, CPT has poor delivery to tumors and low water solubility, limiting its systemic use in cancer therapy.

Use of new nanocarriers allows for the design of secure and efficient multifunctional nanoplatforms for accurate drug

delivery and effective cancer treatment. As a new metal-organic framework (MOF), ZIF-8 has good drug delivery properties and biocompatibility (17–21). Compared to other metal-organic framework (MOF) materials (22–26), ZIF-8 has several unique characteristics. ZIF-8 comprises 2-methylimidazole and  $Zn^{2+}$ . Zinc is the second most abundant transition metal in biology, while biogenic amino acid histidine contains an imidazole group (27). ZIF-8 has exceptional chemical and thermal stability, particularly in aqueous conditions; high specific surface area; and negligible physiological toxicity (28). Moreover, decomposition occurs easily under acidic conditions (pH 5.0–6.0), making ZIF-8 suitable for stimulus-responsive controlled drug release of payloads in the acidic tumor microenvironments (18). ZIF-8 is thus an ideal template for preparing hollow nanomaterials with adjustable sizes for small-molecule drug delivery. The ZIF-8-loaded drugs are less likely to leak during transit to their site of action, retaining pharmaceutical activity until they reach their target tumors (29, 30). Efficient delivery of CPT/MnCO using ZIF-8 nano-frameworks is expected to overcome many limitations of current CO gas therapy.

We designed a therapeutic strategy that combines chemotherapy drug CPT and CO gas prodrug MnCO in a ZIF-8 nanocarrier with good drug delivery properties forming a composite system we named ZCM (**Scheme 1**). After intravenous injection, ZCM circulates systemically, reaching the tumor target, where it is endocytosed. Subsequently, CPT and MnCO are released in response to the acidic tumor microenvironment, where CPT also acts as a  $H_2O_2$  generator increasing the concentration of  $H_2O_2$  in the tumor, synergistically improving the anticancer activity of MnCO. MnCO reacts with  $H_2O_2$  to generate CO *in situ*, directly damaging mitochondria. *In vitro* and *in vivo* experiments indicate that the ZCM system has a high antitumor effect and does not induce significant off-target toxicity, since ZCM does not leak MnCO. The development of ZCM highlights a powerful new approach to MOF-based nanomedicines.

## RESULTS AND DISCUSSION

ZIF-8 nanomaterials of approximately 100 nm were prepared using a simple stirring method (30). Then ZCMs were

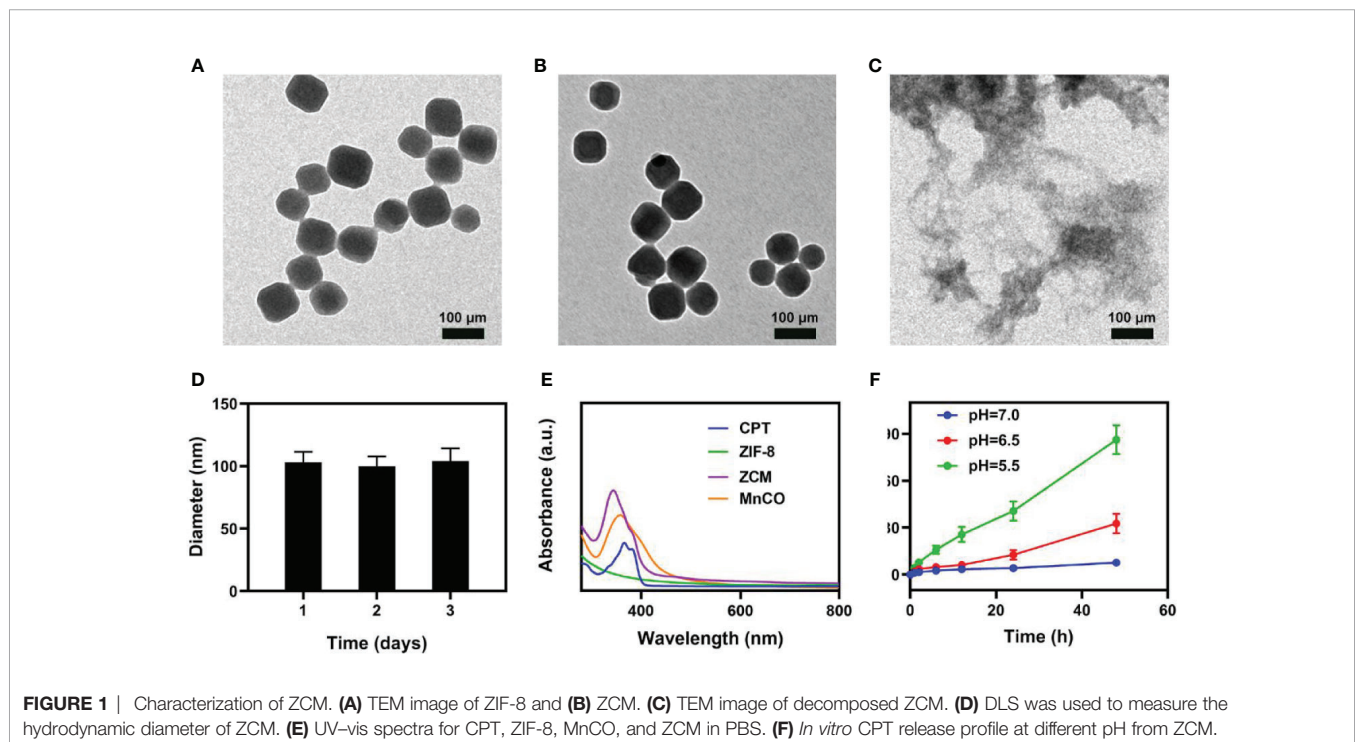


**SCHEME 1** | Illustration of a novel  $H_2O_2$  generator for enhanced CO gas therapy.

synthesized by simultaneous embedment of CPT and MnCO into ZIF-8 to form a ZCM system, as shown in **Figures 1A, B** for transmission electron microscope (TEM) images of pure ZIF-8 and ZCM. A TEM image of ZCM, as measured in an acidic environment (**Figure 1C**), suggests that ZCM can decompose in an acidic environment. The diameter of ZCM (**Figure 1D**) showed almost no changes, again indicating that ZCM was stable and did not alter due to inclusion of drugs. The absorption of CPT, ZIF-8, MnCO, and ZCM was measured using UV-vis absorption spectroscopy, with results indicating the successful preparation of ZCM (**Figure 1E**). The drug loading efficiency of CPT and MnCO in ZCM was found to be 14.6% and 17.8%. ZCM's drug release ability was also studied (**Figure 1F**). Under neutral conditions, ZCM did not decompose and CPT was not released. At pH = 6.5, after 48 h of coculture, CPT release was approximately 30%. At pH = 5.5, CPT release was approximately 38% at 24 h; after 48 h, this had reached almost 90%, with the CPT almost completely released. As shown in **Figure S1**, the release rate of CO rapidly enhances with increasing H<sub>2</sub>O<sub>2</sub> concentrations. This indicated that ZCM can release CO in response to the tumor microenvironment. This indicates that ZCM can help control payload release in the tumor environment, which is expected to alter the tumor microenvironment and realize CO gas therapy.

Our ZCM system performs well, and we are actively conducting *in vitro* antitumor trials. Although MnCO greatly inhibits tumors, the CO yield generated by the H<sub>2</sub>O<sub>2</sub>-MnCO reaction is affected by the H<sub>2</sub>O<sub>2</sub> concentration in the tumor: at 50–100 μM, this is higher than in ordinary cells, but is still limited. Therefore, it is necessary to increase the tumor H<sub>2</sub>O<sub>2</sub> concentration. Our system contains the chemotherapeutic drug

CPT, which produces H<sub>2</sub>O<sub>2</sub>. We verified the ability of ZCM to produce CO; see **Figures 2A, D**. The control group and single ZIF-8 or ZC showed no fluorescence, suggesting a low intracellular CO concentration. ZM containing MnCO shows weak fluorescence. The green fluorescence of the ZCM treatment group was the strongest, since CPT can generate H<sub>2</sub>O<sub>2</sub> in TME, promoting the reaction between MnCO and H<sub>2</sub>O<sub>2</sub>. Changes in mitochondrial membrane potential (MMP) in tumor cells were monitored using the JC-1(5,5',6,6'-tetrachloro-1,1',3,3'-tetraethylimidocarbocyanine) probe method. Typically, JC-1 dye accumulates in the mitochondria, where it aggregates, producing a red fluorescence. However, in damaged mitochondria where MMP is reduced, monomeric dye is released into the cytoplasm, producing green fluorescence. **Figures 2B, E** shows the high green/red fluorescence ratio of cells treated with ZCM. This is consistent with reduced mitochondrial damage due to ZCM. Once ZCM is decomposed by the acidic environment of tumor cells, MnCO will react with H<sub>2</sub>O<sub>2</sub> in TME to produce CO gas *in situ*. This causes serious mitochondrial damage. In addition, we measured the ROS content of different formulations: the ZCM group had high fluorescence, while that of the ZC and ZM groups was much lower (**Figure 2C**). This may be because CPT alters the tumor microenvironment and MnCO produces elevated ROS. ROS can degrade cellular protein and DNA, thus killing tumor cells (27, 31–33). An MTT assay test indicated that the cell viability of the control and ZIF-8 groups was minimally affected, while ZC alone or ZM induced moderate tumor growth inhibition (**Figure 2F**). Our ZCM system showed the greatest tumor inhibition, reaching 90%. There are significant differences when compared to other experimental groups, suggesting that ZCM-



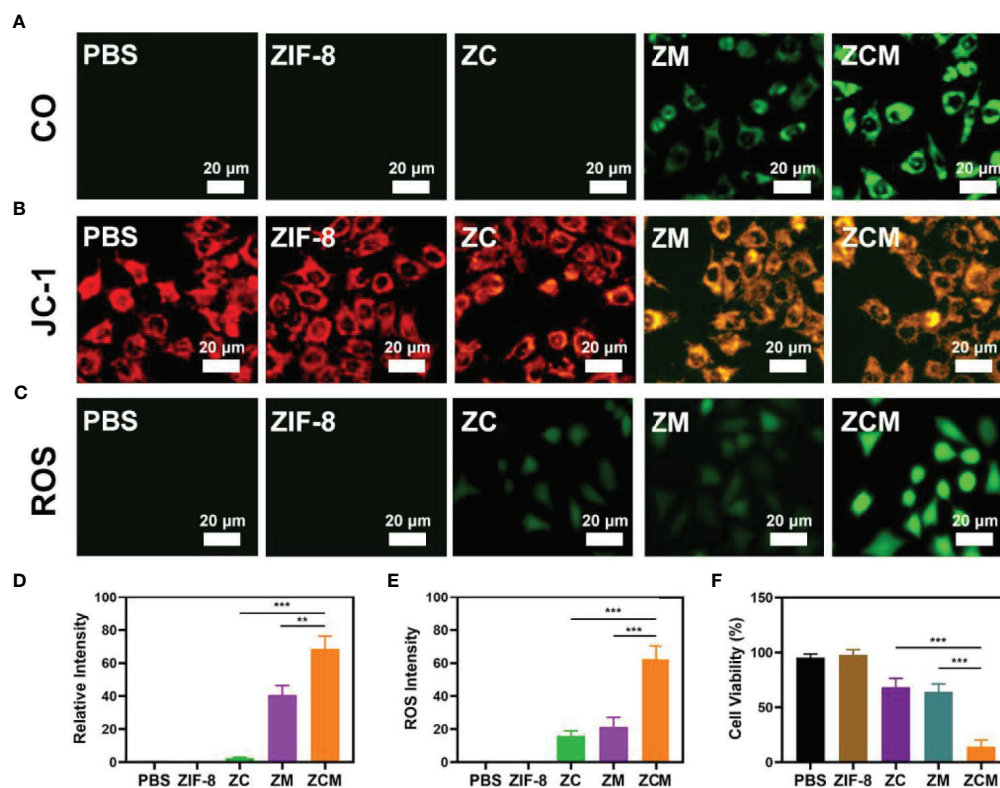


**FIGURE 2** | *In vitro* synergistic therapeutic effects of the ZCM. (A–C) CO (FL-CO-1), JC-1 (green for JC-1 monomer and red for JC-1 aggregate), and ROS (DCFH-DA) fluorescence images under different treatments. (D) Quantification analysis of CO (A) based on the relative intensity of counts of at least 100 cells per treatment group (n = 3). (E) Fluorescence intensity of ROS in (C) based on the relative intensity of counts of at least 100 cells per treatment group (n = 3). (F) The survival of CT26 cells with different treatments. \*\*p < 0.01, \*\*\*p < 0.005; Student's t-test.

mediated increased H<sub>2</sub>O<sub>2</sub> concentrations of TME can enhance the effect of MnCO, inhibiting tumor growth.

We next evaluated the ZCM-mediated antitumor efficacy in mice with CT26 tumors. To investigate the principal effect of ZCM, BALB/c mice were injected subcutaneously into the right flank with  $1 \times 10^6$  CT26 cells. The mice were treated when the primary tumor volume reached 200 mm<sup>3</sup>. Tumor-bearing mice were randomly divided into five groups (five mice per group): (1) PBS; (2) ZIF-8; (3) ZC; (4) ZM; and (5) ZCM. The equivalent CPT dose was 10 mg/kg in groups 3 and 5. Treatment was conducted every 3 days for 16 days. During treatment, the tumor volumes of the control and ZIF-8 groups rose rapidly, which is shown in **Figures 3A, B**. The ZC or ZM group showed a moderate tumor suppression effect. When ZIF-8 reaches the tumor and is endocytosed, the acidic tumor microenvironment causes the ZIF-8 framework to decompose, releasing its drug payload and inducing a therapeutic effect. The ZCM system had the most marked therapeutic effect, with tumor volume growth almost entirely suppressed during treatment. During this study, no weight changes were detected in the treatment group, indicating no significant systemic toxicity (**Figure 3C**). This is crucial since many treatments have clear systemic toxicity, which significantly decreases their potential utility (34–37). We used

the FL-Co-1 + PdCl<sub>2</sub> fluorescence probe to detect the CO content of tumors, confirming that combining CPT and MnCO in ZCM greatly enhanced CO generation in the tumor. We took tumor tissue sections for staining. H&E, TUNEL, and Ki-67 staining (**Figures 3D, E** and **S2, S3**) confirmed there was significant cell necrosis in the ZCM group. As shown in **Figure 4**, there was likewise no inflammatory damage, and liver and kidney indexes were normal. The *in vivo* results indicate that our novel treatment achieved both good biological safety therapy and increased tumor H<sub>2</sub>O<sub>2</sub> concentration, reinforcing the effect of ZCM with profound CO-based therapy.

## CONCLUSION

We designed a novel H<sub>2</sub>O<sub>2</sub> generator ZCM to realize enhanced CO gas therapy. Encapsulated chemotherapeutic agents CPT and MnCO can increase the concentration of H<sub>2</sub>O<sub>2</sub> in the tumor microenvironment driving CO gas therapy, with an enhanced ability to induce tumor cell apoptosis. The *in vitro* and *in vivo* results indicate our system has an excellent tumor inhibition effect. Our ZCM system exhibited no clear toxicity during

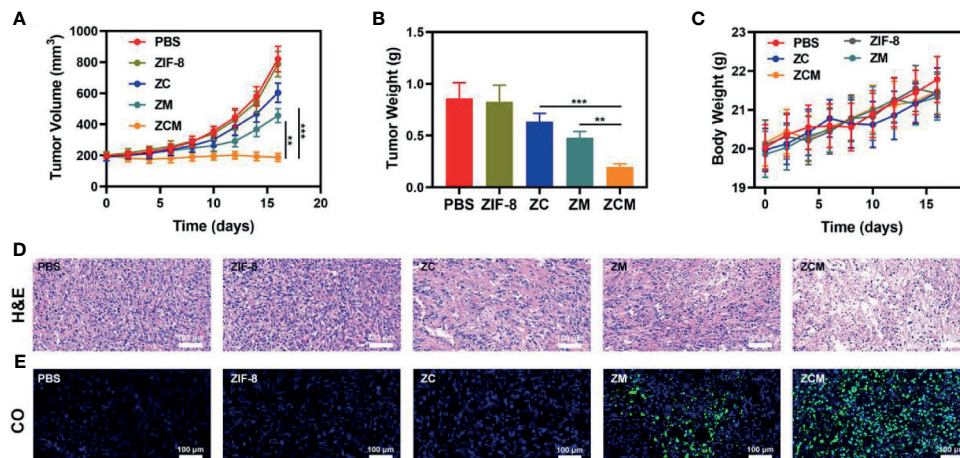


**FIGURE 3** | *In vivo* therapy. (A) Tumor volume, (B) weight, and (C) murine body weight were monitored in the five treatment groups (n = 5). (D) Tumor sections were stained for H&E. (E) Fluorescence imaging for co-localization of the tumor region to test CO production. (Blue: DAPI, green: FL-CO-1). \*\*p < 0.01, \*\*\*p < 0.005; Student's t-test.

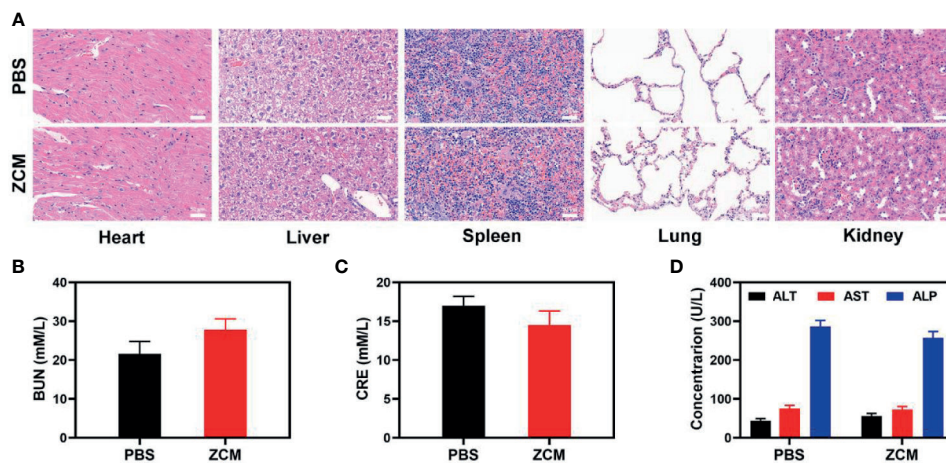


**FIGURE 4** | (A) Histopathologic examination of the tissues including the heart, liver, spleen, lung, and kidney from tumor-bearing mice after PBS or ZCM treatment. (B) Blood biochemistry data for kidney function marker BUN. (C) Blood biochemistry data including kidney function marker CRE. (D) Liver function markers: ALT, AST, and ALP.

treatment. As non-toxic materials have better application potential and will also reduce the pain of patients during treatment. Although many materials have good antitumor effects, their systemic toxicity significantly affects the application value. We will explore the biological application of our combination of MnCO and other novel nanotechnology vehicles, optimizing our treatment plan.

## DATA AVAILABILITY STATEMENT

The raw data supporting the conclusions of this article will be made available by the authors, without undue reservation.

## ETHICS STATEMENT

The animal study was reviewed and approved by the Institutional Animal Care and Use Committee of Wuhan University.

## AUTHOR CONTRIBUTIONS

Conceived and designed the experiments: YL, ZL, and WZ. Performed the experiments: YL, ZL, DJ, YW, KZ, and CL. Contributed reagents/materials/analysis tools: NZ, DJ, YW, KZ, and CL. Revised and polished the article: NZ, YL, ZL, DJ, YW, KZ, and CL. All authors contributed to the article and approved the submitted version.

## FUNDING

This work was supported by the National Natural Science Foundation of China (81901771) and Zhongnan Hospital of Wuhan University Science, Technology and Innovation Seed Fund, Project znp2019022.

## REFERENCES

- Chen Q, Xu L, Liang C, Wang C, Peng R, Liu Z. Photothermal Therapy With Immune-Adjuvant Nanoparticles Together With Checkpoint Blockade for Effective Cancer Immunotherapy. *Nat Commun* (2016) 7:13193. doi: 10.1038/ncomms13193
- Zhang F, Lei Z. Molecular Engineering of NIR-II Fluorophores for Improved Biomedical Detection. *Angewandte Chemie* (2020) 60:16294–308.
- Liang C, Zhang X, Yang M, Wang W, Chen P, Dong X. Remodeling Tumor Microenvironment by Multifunctional Nanoassemblies for Enhanced Photodynamic Cancer Therapy. *ACS Materials Lett* (2020) 2(10):1268–86. doi: 10.1021/acsmaterialslett.0c00259
- Wang J, Sui L, Huang J, Miao L, Nie Y, Wang K, et al. MoS<sub>2</sub>-Based Nanocomposites for Cancer Diagnosis and Therapy. *Bioact Mater* (2021) 6(11):4209–42. doi: 10.1016/j.bioactmat.2021.04.021
- Ai K, Huang J, Xiao Z, Yang Y, Bai Y, Peng J. Localized Surface Plasmon Resonance Properties and Biomedical Applications of Copper Selenide Nanomaterials. *Mater Today Chem* (2021) 20:100402. doi: 10.1016/j.mtchem.2020.100402
- Zhu D, Liu Z, Li Y, Huang Q, Xia L, Li K. Delivery of Manganese Carbonyl to the Tumor Microenvironment Using Tumor-Derived Exosomes for Cancer Gas Therapy and Low Dose Radiotherapy. *Biomaterials* (2021) 274:120894. doi: 10.1016/j.biomaterials.2021.120894
- Wu L, Cai X, Zhu H, Li J, Shi D, Su D, et al. PDT-Driven Highly Efficient Intracellular Delivery and Controlled Release of CO in Combination With Sufficient Singlet Oxygen Production for Synergistic Anticancer Therapy. *Adv Funct Mater* (2018) 28(41):1804324. doi: 10.1002/adfm.201804324
- Wang S, Shang L, Li L, Yu Y, Chi C, Wang K, et al. Metal-Organic-Framework-Derived Mesoporous Carbon Nanospheres Containing Porphyrin-Like Metal Centers for Conformal Phototherapy. *Adv Mater* (2016) 28(38):8379–87. doi: 10.1002/adma.201602197
- Wu D, Duan X, Guan Q, Liu J, Yang X, Zhang F, et al. Mesoporous Polydopamine Carrying Manganese Carbonyl Responds to Tumor Microenvironment for Multimodal Imaging-Guided Cancer Therapy. *Adv Funct Mater* (2019) 29(16):1900095. doi: 10.1002/adfm.201900095
- Jin Z, Wen Y, Xiong L, Yang T, Zhao P, Tan L, et al. Intratumoral H<sub>2</sub>O<sub>2</sub>-Triggered Release of CO From a Metal Carbonyl-Based Nanomedicine for Efficient CO Therapy. *Chem Commun* (2017) 53(40):5557–60. doi: 10.1039/C7CC01576C
- Li WP, Su CH, Chang YC, Lin YJ, Yeh CS. Ultrasound-Induced Reactive Oxygen Species Mediated Therapy and Imaging Using a Fenton Reaction Activable Polymersome. *ACS Nano* (2016) 10(2):2017–27. doi: 10.1021/acsnano.5b06175
- Tang Z, Zhang H, Liu Y, Ni D, Zhang H, Zhang J, et al. Antiferromagnetic Pyrite as the Tumor Microenvironment-Mediated Nanoplateform for Self-Enhanced Tumor Imaging and Therapy. *Adv Mater* (2017) 29(47):1701683. doi: 10.1002/adma.201701683
- Huo M, Wang L, Chen Y, Shi J. Tumor-Selective Catalytic Nanomedicine by Nanocatalyst Delivery. *Nat Commun* (2017) 8(1):357. doi: 10.1038/s41467-017-00424-8
- Tang Y, Lu X, Yin C, Zhao H, Hu W, Hu X, et al. Chemiluminescence-Initiated and in Situ-Enhanced Photoisomerization for Tissue-Depth-Independent Photo-Controlled Drug Release. *Chem Sci* (2019) 10(5):1401–9. doi: 10.1039/C8SC04012E
- Gong L, Zhang Y, Liu C, Zhang M, Han S. Application of Radiosensitizers in Cancer Radiotherapy. *Int J Nanomed* (2021) 16:1083–102. doi: 10.2147/IJN.S290438
- Liang Q, Bie N, Yong T, Tang K, Shi X, Wei Z, et al. The Softness of Tumour-Cell-Derived Microparticles Regulates Their Drug-Delivery Efficiency. *Nat Biomed Eng* (2019) 3(9):729–40. doi: 10.1038/s41551-019-0405-4
- Su L, Wu Q, Tan L, Huang Z, Fu C, Ren X, et al. High Biocompatible ZIF-8 Coated by ZrO<sub>2</sub> for Chemo-Microwave Thermal Tumor Synergistic Therapy. *ACS Appl Mater Interf* (2019) 11(11):10520–31. doi: 10.1021/acsami.8b22177
- Shao F, Wu Y, Tian Z, Liu S. Biomimetic Nanoreactor for Targeted Cancer Starvation Therapy and Cascade Amplified Chemotherapy. *Biomaterials* (2021) 274:120869. doi: 10.1016/j.biomaterials.2021.120869
- Maleki A, Shahbazi MA, Alinezhad V, Santos HA. The Progress and Prospect of Zeolitic Imidazolate Frameworks in Cancer Therapy, Antibacterial Activity, and Biomineralization. *Advanced Healthcare Mater* (2020) 9(12):e2000248. doi: 10.1002/adhm.202000248
- Meng X, Jia K, Sun K, Zhang L, Wang Z. Smart Responsive Nanoplateform via in Situ Forming Disulfiram-Copper Ion Chelation Complex for Cancer Combination Chemotherapy. *Chem Eng J* (2021) 415. doi: 10.1016/j.cej.2021.128947
- Geng S, Lou R, Yin Q, Li S, Yang R, Zhou J. Reshaping the Tumor Microenvironment for Increasing the Distribution of Glucose Oxidase in Tumor and Inhibiting Metastasis. *J Mater Chem B* (2021) 9(5):1424–31. doi: 10.1039/D0TB02468F
- Huang C, Ding S, Jiang W, Wang FB. Glutathione-Depleting Nanoplatelets for Enhanced Sonodynamic Cancer Therapy. *Nanoscale* (2021) 13:4512–8. doi: 10.1039/D0NR08440A
- Yang G, Xu L, Chao Y, Xu J, Sun X, Wu Y, et al. Hollow MnO<sub>2</sub> as a Tumor-Microenvironment-Responsive Biodegradable Nano-Platform for Combination Therapy Favoring Antitumor Immune Responses. *Nat Commun* (2017) 8(1):902. doi: 10.1038/s41467-017-01050-0
- Fan W, Bu W, Shen B, He Q, Cui Z, Liu Y, et al. Intelligent MnO<sub>2</sub> Nanosheets Anchored With Upconversion Nanoprobes for Concurrent pH-/H<sub>2</sub>O<sub>2</sub>-Responsive UCL Imaging and Oxygen-Elevated Synergetic Therapy. *Adv Mater* (2015) 27(28):4155–61. doi: 10.1002/adma.201405141
- Zhu Y, Shi H, Li T, Yu J, Guo Z, Cheng J, et al. A Dual Functional Nanoreactor for Synergistic Starvation and Photodynamic Therapy. *ACS Appl Mater Interf* (2020) 12(16):18309–18. doi: 10.1021/acsami.0c01039
- Song C, Xu W, Wei Z, Ou C, Wu J, Tong J, et al. Anti-LDLR Modified TPZ@Ce6-PEG Complexes for Tumor Hypoxia-Targeting Chemo-/Radio-/Photodynamic/Photothermal Therapy. *J Mater Chem B* (2020) 8(4):648–54. doi: 10.1039/C9TB02248A
- Liu X, Liu Z, Dong K, Wu S, Sang Y, Cui T, et al. Tumor-Activatable Ultrasmall Nanozyme Generator for Enhanced Penetration and Deep Catalytic Therapy. *Biomaterials* (2020) 258:120263. doi: 10.1016/j.biomaterials.2020.120263
- Li Y, Xu N, Zhu W, Wang L, Liu B, Zhang J, et al. Nanoscale Melittin@Zeolitic Imidazolate Frameworks for Enhanced Anticancer Activity and Mechanism Analysis. *ACS Appl Mater Interf* (2018) 10(27):22974–84. doi: 10.1021/acsami.8b06125
- Zhao Q, Gong Z, Li Z, Wang J, Zhang J, Zhao Z, et al. Target Reprogramming Lysosomes of CD8<sup>+</sup> T Cells by a Mineralized Metal-Organic Framework for Cancer Immunotherapy. *Adv Mater* (2021) 30:2100616. doi: 10.1002/adma.202100616
- Li S, Tan L, Meng X. Nanoscale Metal-Organic Frameworks: Synthesis, Biocompatibility, Imaging Applications, and Thermal and Dynamic Therapy of Tumors. *Adv Funct Mater* (2020) 30(13):1908924. doi: 10.1002/adfm.201908924
- Ding S, Liu Z, Huang C, Zeng N, Jiang W, Li Q. Novel Engineered Bacterium/Black Phosphorus Quantum Dot Hybrid System for Hypoxic Tumor Targeting and Efficient Photodynamic Therapy. *ACS Appl Mater Interf* (2021). doi: 10.1021/acsami.0c20254
- Zhang C, Yan L, Gu Z, Zhao Y. Strategies Based on Metal-Based Nanoparticles for Hypoxic-Tumor Radiotherapy. *Chem Sci* (2019) 10(29):6932–43. doi: 10.1039/C9SC02107H

## SUPPLEMENTARY MATERIAL

The Supplementary Material for this article can be found online at: <https://www.frontiersin.org/articles/10.3389/fonc.2021.738567/full#supplementary-material>

33. Chang M, Hou Z, Wang M, Yang C, Wang R, Li F, et al. Single-Atom Pd Nanozyme for Ferroptosis-Boosted Mild-Temperature Photothermal Therapy. *Angewandte Chemie* (2021) 60(23):12971–9. doi: 10.1002/anie.202101924
34. Guo B, Wu M, Shi Q, Dai T, Xu S, Jiang J, et al. All-In-One Molecular Aggregation-Induced Emission Theranostics: Fluorescence Image Guided and Mitochondria Targeted Chemo- and Photodynamic Cancer Cell Ablation. *Chem Mater* (2020) 32(11):4681–91. doi: 10.1021/acs.chemmater.0c01187
35. Yu W, Liu T, Zhang M, Wang Z, Ye J, Li CX, et al. O<sub>2</sub> Economizer for Inhibiting Cell Respiration To Combat the Hypoxia Obstacle in Tumor Treatments. *ACS Nano* (2019) 13(2):1784–94. doi: 10.1021/acsnano.8b07852
36. Zhu D, Zhang J, Luo G, Duo Y, Tang BZ. Bright Bacterium for Hypoxia-Tolerant Photodynamic Therapy Against Orthotopic Colon Tumors by an Interventional Method. *Adv Sci* (2021) (8):2004769. doi: 10.1002/advs.202004769
37. Huang C, Chen B, Chen M, Jiang W, Liu W. Injectable Hydrogel for Cu(2+) Controlled Release and Potent Tumor Therapy. *Life (Basel)* (2021) 11(5):391. doi: 10.3390/life11050391

**Conflict of Interest:** The authors declare that the research was conducted in the absence of any commercial or financial relationships that could be construed as a potential conflict of interest.

**Publisher's Note:** All claims expressed in this article are solely those of the authors and do not necessarily represent those of their affiliated organizations, or those of the publisher, the editors and the reviewers. Any product that may be evaluated in this article, or claim that may be made by its manufacturer, is not guaranteed or endorsed by the publisher.

Copyright © 2021 Li, Liu, Zeng, Wang, Liu, Zeng, Zhong, Jiang and Wu. This is an open-access article distributed under the terms of the Creative Commons Attribution License (CC BY). The use, distribution or reproduction in other forums is permitted, provided the original author(s) and the copyright owner(s) are credited and that the original publication in this journal is cited, in accordance with accepted academic practice. No use, distribution or reproduction is permitted which does not comply with these terms.